

# The Role of Specific Side Groups and pH in Magnetization Transfer in Polymers

D. F. Gochberg,<sup>1</sup> R. P. Kennan, M. J. Maryanski,<sup>2</sup> and J. C. Gore

*Department of Diagnostic Radiology, Yale University School of Medicine, 333 Cedar St., Fitkin B, New Haven, Connecticut 06510*

Received August 4, 1997; revised January 6, 1998

**The nature of water–macromolecule interactions in aqueous model polymers has been investigated using quantitative measurements of magnetization transfer. Cross-linked polymer gels composed of 94% water, 3% *N,N'*-methylene-bis-acrylamide, and 3% functional monomer (acrylamide, methacrylamide, acrylic acid, methacrylic acid, 2-hydroxyethyl-acrylate, or 2-hydroxyethyl-methacrylate) were studied. Water–macromolecule interactions were modified by varying the pH and specific functional group on the monomer. The magnitudes of the interactions were quantified by measuring the rate of proton nuclear spin magnetization exchange between the polymer matrix and the water. This rate was highly sensitive to the presence of carboxyl side groups on the macromolecule. However, the dependence of the rate on pH was not consistent with simple acid/base-catalyzed chemical exchange, and instead, the data suggest that multiequilibria proton exchange, a wide distribution in surface group p*K* values, and/or a macromolecular structural dependence on pH may play a significant role in magnetization transfer in polymer systems. These model polymer gels afford useful insights into the relevance of chemical composition and chemical dynamics on relaxation in tissues.** © 1998 Academic Press

**Key Words:** MT; cross-relaxation; relaxation; biopolymers; exchange.

## INTRODUCTION

There are several aspects of the details of proton relaxation in biological tissues that are poorly understood, and quantitative models that could be used to explain biological changes are still elusive. A more complete understanding of proton relaxation in tissue could affect the interpretation of clinical MR images used every day for radiological diagnosis, could provide a better comprehension of the use and limitations of quantitative NMR parameters, and might suggest new methods of contrast manipulation. In order to better elucidate the nature of interactions between macromolecules and water, recent work (1–6) has focused on measurements of magnetization transfer and the field dispersion of relaxation rates.

Many of these studies have used biopolymers such as agarose and albumin as prototype systems, which reproduce many of the features of relaxation found in tissue. Unfortunately these molecules are inherently complex and interpretations of the data are not always straightforward. They are also limited in terms of what variations of composition can be achieved. Although water relaxation in solutions of diamagnetic proteins is relatively well documented, there is a growing realization that tissue relaxation cannot be considered a simple sum of the effects of isolated macromolecules (7). Instead the dominant relaxation effect comes from supramolecular organization, such as distinguishes solutions of albumin from their heat-treated and cross-linked counterparts (3). The mechanism by which this magnetization transfer occurs, and its dependence on the rigidity and composition of the matrix, is not well understood. Two competing views have emphasized either the role of proton chemical exchange (8, 9) or that of interfacial solvent protons (“bound water”) (3) as conduits for spin exchange. We have therefore sought to study simple polymer systems which show many relaxation and magnetization transfer (MT) properties that are similar to biological tissue but in which aspects of the composition can be controlled.

In a previous study (10) we reported the effects of the degree of cross-linking and matrix rigidity on the efficacy of MT. In this paper we report the results of studies on similar polymer gels which share many common structural features, but in which the surface groups exposed to solvent water and the pH have been independently controlled.

## MATERIALS

NMR studies were performed on polymer gels which were prepared from varying mixtures of comonomers (6% by weight total monomer: 94% water) which contained different chemical groups. The monomers formed a polymer cross-linked with *N,N'*-methylene-bis-acrylamide (BIS). The fractional composition of BIS and monomer was 50:50 (i.e., 3% BIS and 3% monomer). The resultant polymers contained a variety of surface groups found in biological materials: amide groups (from

<sup>1</sup> Also Department of Physics, Yale University.

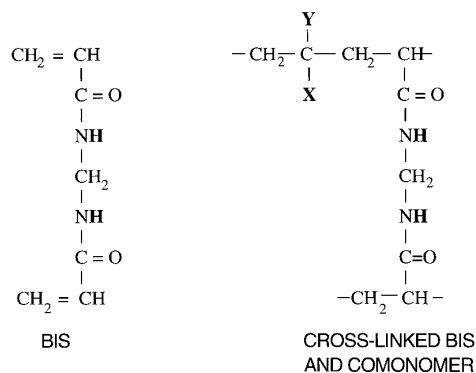
<sup>2</sup> Also MGS Research Inc., P.O. Box 581, Guilford, CT 06437-0581.

using acrylamide or methacrylamide as monomers), carboxyl groups (acrylic acid, methacrylic acid), and esters with an exchanging OH group (2-hydroxyethyl-acrylate, 2-hydroxyethyl-methacrylate). Figure 1 illustrates a section of a polymer showing how BIS forms cross-links between chains of the monomer. Depending on the monomer, the surface groups of the polymer will vary, as indicated by  $X$  and  $Y$  in Fig. 1 and Table 1. The variation in  $X$  changes the putative active site for spin exchange, as indicated in Table 1. The variation in  $Y$  controls the presence of a  $\text{CH}_3$  spin relaxation sink in the macromolecule.

Polymerization was initiated under nitrogen at  $50^\circ\text{C}$ , using ammonium persulfate and sodium thiosulfate. pH was adjusted by soaking the cross-linked polymer in buffer. By manipulating the pH after the gel has been cross-linked, it is hoped that the macromolecular structure does not have a significant pH dependence. This issue will be addressed under Discussion. Details of the gel preparation have been previously described elsewhere (10). The measured pH of the buffer changed by no more than 0.3 pH unit before and after soaking the gel. The gel was dried after soaking until the original weight was regained.

## METHODS

The degree and rates of magnetization transfer in the polymers were quantified by measuring the rapid response of the mobile proton pool to a selective inversion-recovery pulse



EXAMPLE:

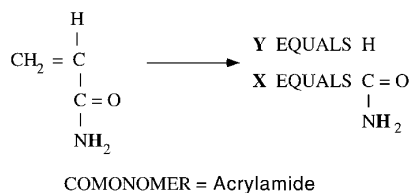


**FIG. 1.** The polymer gels are composed of 94% water, 3% BIS, and 3% comonomer. As the comonomer is varied,  $X$  and  $Y$  change as documented in Table 1. An example is given for acrylamide.

**TABLE 1**

Comonomer	Putative active site	X	Y
Acrylamide	$\text{NH}_2$	$\text{C}=\text{O}$   $\text{NH}_2$	H
Methacrylamide	$\text{NH}_2$	$\text{C}=\text{O}$   $\text{NH}_2$	$\text{CH}_3$
Acrylic acid	$\text{C}=\text{O}$   $\text{OH}$	$\text{C}=\text{O}$   $\text{OH}$	H
Methacrylic acid	$\text{C}=\text{O}$   $\text{OH}$	$\text{C}=\text{O}$   $\text{OH}$	$\text{CH}_3$
2-Hydroxyethyl-acrylate	$\text{OH}$	$\text{C}=\text{O}$   O   $\text{CH}_2$   $\text{CH}_2\text{OH}$	H
2-Hydroxyethyl-methacrylate	$\text{OH}$	$\text{C}=\text{O}$   O   $\text{CH}_2$   $\text{CH}_2\text{OH}$	$\text{CH}_3$

*Note.* The polymer gels are composed of 94% water, 3% BIS, and 3% comonomer. As the comonomer is varied,  $X$  and  $Y$  in Fig. 1 change as indicated above.

sequence. The experimental details of this sequence have been described previously (11). The recovery of the mobile proton pool after inversion is analyzed to quantify the rate of MT. In the present work, phase cycling and homospoil gradient pulses were used in conjunction to attenuate the wiggles superimposed on the biexponential recovery by the effects of residual transverse magnetization (11). A  $700\text{-}\mu\text{s}$  inversion pulse was used, which effectively inverted the mobile proton pool ( $T_2 \sim 100\text{ ms}$ ) without affecting the immobile proton pool ( $T_2 \sim 10\text{ }\mu\text{s}$ ). The response of the signal from the mobile proton pool to such a sequence was then analyzed in terms of two compartments coupled by exchange. The two pools comprise the free, mobile water protons whose resonance is motionally narrowed, and a second proton pool corresponding to macromolecular protons that are relatively immobile and hence show broad resonances. This model is described in more detail below.

The evolution of the mobile water proton signal (when there is no applied radiofrequency radiation) is then given by (12, 13)

$$\frac{M_f(t)}{M_{f\infty}} = b_f^+ \exp(-R_f^+ t) + b_f^- \exp(-R_f^- t) + 1, \quad [1]$$

where

$$2R_1^\pm = R_{1f} + R_{1m} + k_{fm} + k_{mf} \pm \sqrt{(R_{1f} - R_{1m} + k_{fm} - k_{mf})^2 + 4k_{fm}k_{mf}} \quad [2]$$

$$b_f^\pm = \pm \left( \left[ \frac{M_f(0) - M_{f\infty}}{M_{f\infty}} \right] (R_{1f} - R_1^\mp) + \left[ \frac{M_f(0)}{M_{f\infty}} - \frac{M_m(0)}{M_{m\infty}} \right] k_{fm} \right) \frac{1}{R_1^+ - R_1^-} \quad [3]$$

$M_f(t)$  is the longitudinal magnetization of the mobile protons at time  $t$ , whose equilibrium value is  $M_{f\infty}$ .  $R_{1f}$  and  $R_{1m}$  are the longitudinal relaxation rates of the mobile and macromolecular protons when there is no magnetization transfer between them, and  $k_{mf}$  and  $k_{fm}$  are the rates of magnetization transfer between them. The subscripts  $f$  and  $m$  refer to the free solvent and macromolecular (immobile) proton pools, respectively.  $R_1^-$  is the slow recovery rate, which is often referred to as the measured value of  $R_1$ .  $R_1^+$  is a fast recovery rate. For the case of  $k_{mf}$  much greater than all other terms in Eq. [2], as is commonly found in macromolecular structures,  $R_1^+ \approx k_{mf}$ .

Selective inversion-recovery measurements with variable delays between the  $180^\circ$  and  $90^\circ$  pulses were performed to

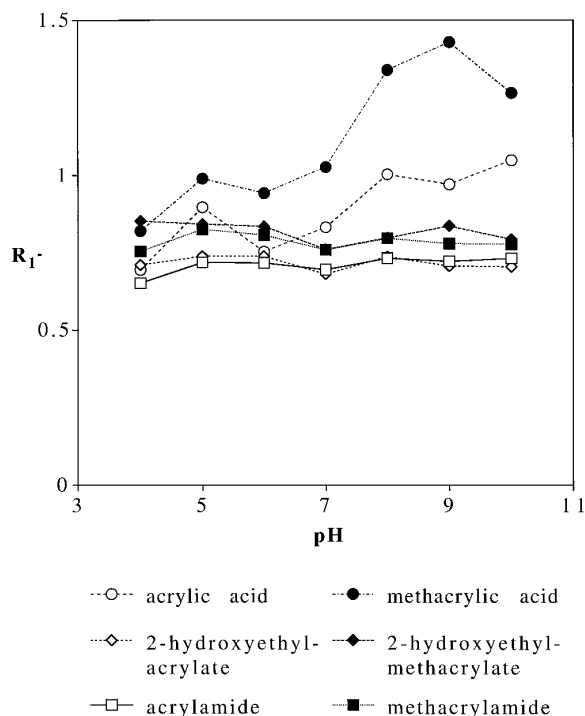


**FIG. 3.**  $R_1^-$  vs pH for BIS gels with varied comonomers. The error bars as determined from the diagonal elements of the covariance matrix are too small to be visible. No attempt was made to determine the errors resulting from sample variation.

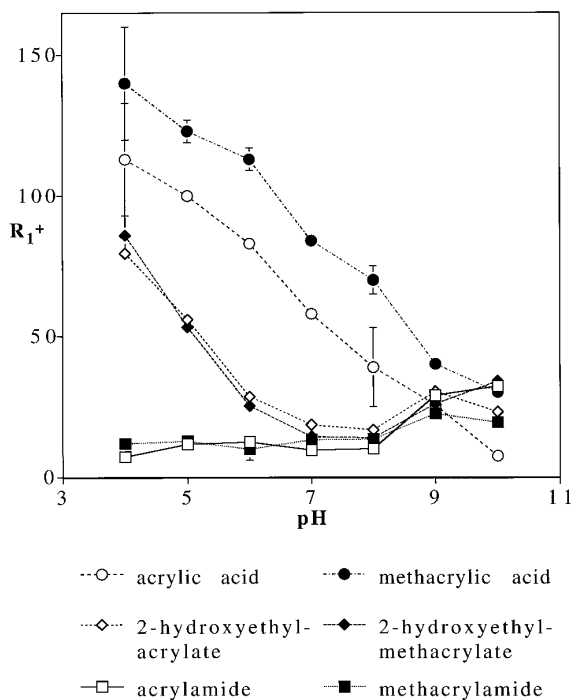


**FIG. 2.**  $R_1^+$  vs pH for BIS gels with varied comonomers. The error bars come from the diagonal elements of the covariance matrix (28).

obtain  $R_1^+$  and  $R_1^-$ . A least-squares fit gave two rate constants. In addition,  $R_2$  was measured for each sample using a Carr-Purcell-Meiboom-Gill sequence with  $180^\circ$  pulses spaced by 4 ms. All measurements were made using a 2-T GE CSI spectrometer, using a solenoid RF coil of 12.8 mm inside diameter on samples inside glass culture tubes of 8.5 mm inside diameter.

## RESULTS

Figures 2 through 4 give  $R_1^+$ ,  $R_1^-$ , and  $R_2$  as a function of pH for each of the six polymers. The key results are: (1) the significant dependence of  $R_1^+$  on the polymer side group, especially the presence of carboxyls; (2) the qualitative similarity in the  $R_1^+$  and  $R_2$  dependencies on chemical composition and pH; and (3) the smaller and less definite changes in  $R_1^-$  in comparison to the changes in  $R_1^+$  and  $R_2$ . Each of these points will be examined under Discussion. In addition, this section will apply the quantitative model of spin exchange outlined under Theory to the gels with carboxyl side groups.

## THEORY

Mobile protons within a system exhibiting MT may exchange spin via protons within the solvent-matrix interface

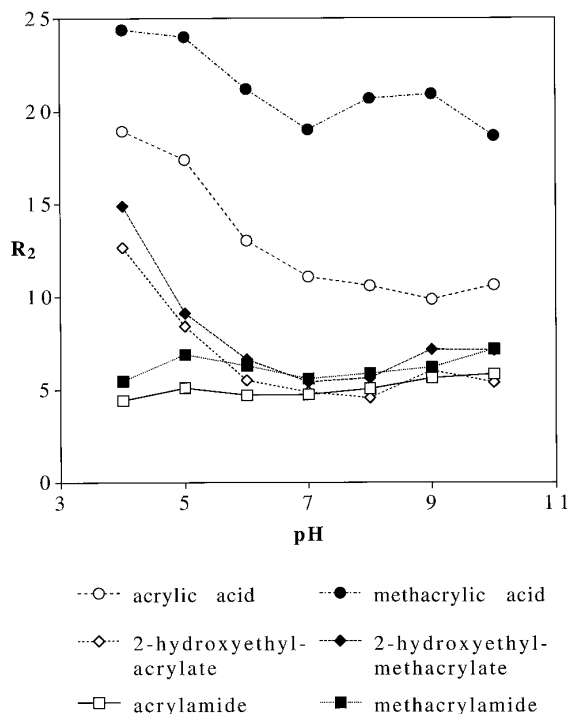


**FIG. 4.**  $R_2$  vs pH for BIS gels with varied comonomers. The error bars as determined from the diagonal elements of the covariance matrix are too small to be visible. No attempt was made to determine the errors resulting from sample variation.

and via dissociable protons on the matrix. Each of these intermediate pathways may be represented by several separate proton pools, each being described by its own size and spin exchange rates. Koenig (14), for example, models bound water as consisting of several separate pools, each with a different residence time. A general case is illustrated in Fig. 5. Unfortunately, such models have too many free parameters to be measured experimentally, and its current use is for illustrative purposes only. All spin exchange on the right half of the figure occurs via chemical exchange. All spin exchange on the left half of the figure occurs via dipole-dipole interactions. All interactions between different intermediate proton pools are ignored. Note that exchange via any conduit is assumed to share common features: (1) a proton diffuses from the free solvent to the macromolecular interface; (2) the proton is held at the interface either by being part of a water molecule that binds for some time or after chemical exchange at a specific site; and (3) the proton may then exchange spin with an adjacent macromolecular proton via a dipole-dipole interaction. Because of the parallel nature of the interactions, a single MT experiment cannot, in and of itself, distinguish between the different mechanisms.

In this work, the overall effective spin exchange between the nonexchangeable macromolecular protons and the free solvent protons is detected. The measured signal recovery

is well fit by a biexponential, consistent with a model of exchange with no intermediate pools. In the present case, there exists at least one intermediate pool, as illustrated in Fig. 6, and a theoretical connection to an apparent two-pool system is needed.

In the absence of RF pulses the dynamics of a spin system as shown in Fig. 6 are described by coupled differential equations,

$$\begin{aligned} \frac{d}{dt} \begin{bmatrix} M_f(t) \\ M_i(t) \\ M_m(t) \end{bmatrix} &= \begin{bmatrix} -(R_{1f} + k_{fi}) & k_{if} & 0 \\ k_{fi} & -(R_{1i} + k_{if} + k_{im}) & k_{mi} \\ 0 & k_{im} & -(R_{1m} + k_{mi}) \end{bmatrix} \\ &\times \begin{bmatrix} M_f(t) \\ M_i(t) \\ M_m(t) \end{bmatrix} + \begin{bmatrix} R_{1f}M_{f\infty} \\ R_{1i}M_{i\infty} \\ R_{1m}M_{m\infty} \end{bmatrix}, \end{aligned} \quad [4]$$

where  $M_f(t)$ ,  $M_i(t)$ , and  $M_m(t)$  are the instantaneous longitudinal magnetizations, and  $M_{f\infty}$ ,  $M_{i\infty}$ , and  $M_{m\infty}$  are proportional to the proton fractions  $p_f$ ,  $p_i$ , and  $p_m$ , respectively. The subscripts f, i, and m refer to the free solvent, intermediate, and nonexchangeable proton pools, respectively. In general, these equations lead to triexponential recovery toward

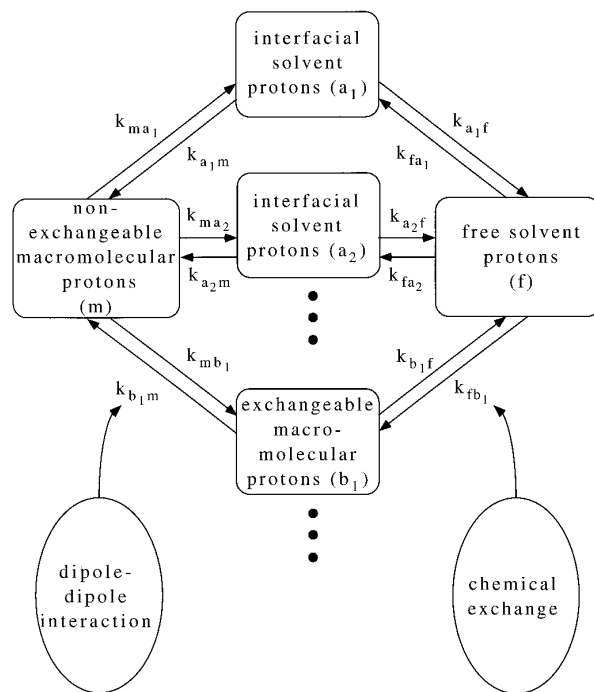


**FIG. 5.** A model for magnetization transfer in heterogeneous systems.

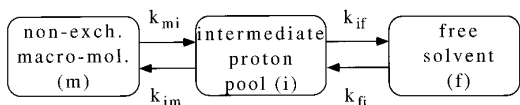


FIG. 6. A model for magnetization transfer with a single, unspecified intermediate proton pool.

equilibrium for all three proton pools. Under certain conditions, however, this system will act like a two-pool system with biexponential recovery.

For a small intermediate pool, the effective two-pool spin exchange rate from pool ‘‘m’’ to pool ‘‘f’’ is

$$k_{mf, \text{effective}} = \frac{p_i k_{im} k_{if}}{p_m (k_{im} + k_{if})}, \quad [5]$$

$$= \frac{p_i k_{im}}{p_m}, \quad \text{when } k_{im} \ll k_{if} \quad [6]$$

$$= \frac{p_i k_{if}}{p_m}, \quad \text{when } k_{if} \ll k_{im}. \quad [7]$$

This value of  $k_{mf, \text{effective}}$  can be derived in two ways: (1) by equating the total time for spin exchange to the sum of the intermediate exchange times (13); and (2), more rigorously, by assuming that  $d/dt M_i(t) \ll k_{mi} M_m(t)$ ,  $k_{fi} M_f(t)$  and that  $R_{ii} \ll k_{if}$ ,  $k_{im}$  in Eq. [4].

The effect of magnetization transfer on transverse relaxation is more complicated. Figure 7 depicts this process, showing that cross-relaxation effects from the dipole–dipole interaction are ignored. Ignoring mutual spin flips is justified when there exist differences in the precession frequencies of the transverse magnetization. A more rigorous analysis of transverse relaxation in such a spin system may include cross-relaxation terms as applicable to nearly like spins (15, 16). Such an analysis, however, goes beyond the current work.

The macromolecular protons do affect the transverse relaxation of the intermediate proton pool and, indirectly, the free solvent. Assuming that  $p_i \ll p_f$  and  $R_{2i} \gg R_{2f}$ , there are two relevant cases. First, when  $k_{im} \ll k_{if}$ , the observed relaxation rate of the solvent proton pool is of the order (13)

$$R_2 = R_{2f} + \frac{p_i}{p_f} \frac{5}{2} k_{im}, \quad [8]$$

where  $R_{2f}$  is the sum of all other relaxation effects on the intermediate proton pool, including hydrodynamic effects caused by the macromolecule. Second, when  $k_{if} \ll k_{im}$ , the transverse relaxation is exchange rate limited. The resulting relaxation is (13, 17)

$$R_2 = R_{2f} + \frac{p_i}{p_f} k_{if}. \quad [9]$$

This connection between the transverse relaxation rate of the water and the longitudinal rate of MT is due to their similar dependencies on the frequency of the dipole–dipole interaction between the intermediate and macromolecular proton pools (13).

The effects of any Larmor frequency separations between the exchanging sites have been ignored in the above analysis. If  $R_{2i}$  is much larger than the difference in the Larmor frequencies (as should be the case for our samples), the effects of such frequency separations in a CPMG experiment are negligible (18). Previous measurements of similar gels showed that  $R_2$  depended on the CPMG pulse spacing, indicating the presence of exchanging proton pools with a smaller  $R_2$  value. Such intermediate proton pools are ignored in the present analysis of magnetization transfer, since the motional narrowing which makes  $R_2$  small will also make cross-relaxation inefficient.

The above descriptions of the effects of a macromolecular proton pool on longitudinal spin exchange and transverse spin relaxation can be combined. Any process which changes  $p_i$ ,  $k_{im}$ , and  $k_{if}$  only will affect the ratios

$$\frac{\Delta k_{mf, \text{effective}}}{\Delta R_2} = \frac{p_f}{p_m}, \quad \text{when } k_{if} \ll k_{im} \quad [10]$$

$$= \frac{2}{5} \frac{p_f}{p_m}, \quad \text{when } k_{im} \ll k_{if}, \quad [11]$$

where  $\Delta k_{mf, \text{effective}}$  and  $\Delta R_2$  are the changes in the measured rates. This result can be used to interpret the changes seen in the samples measured here.

## DISCUSSION

The most striking experimental result is the large dependence of  $R_1^+$  on the precise nature of the side group of the polymer. Since  $R_1^+ \approx k_{mf}$ , this clear dependence of the rate of magnetization transfer supports the view that certain side groups are key conduits for MT in tissue. Specifically,  $R_1^+$  is, at physiologic pH, very sensitive to the presence of carboxyl groups, especially when there are also present free methyl groups that may act as relaxation sinks. Previous studies (19–21) have focused on the presence of OH groups

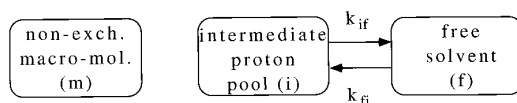


FIG. 7. A model for transverse relaxation.

in lipids, finding a rough proportionality between the OH group surface density and the MT rate (21). In distinction, the present work suggests that there may be a strong dependence on carboxyl group density in biomolecules, as also suggested elsewhere (14). (These comparisons between gels with different structures should be taken as guidelines only.) Note that, in the current work, the  $R_1^+$  value of 2-hydroxyethyl-acrylate (which has an exchanging OH group) is significantly less than the carboxyl carrying acrylic acid. Also note that the  $R_1^+$  values of acrylamide and methacrylamide (the amides) increase significantly around 8 pH units. A similar pH-dependent increase in MT was previously measured in 100% BIS gels (10). The  $R_1^+$  values of 2-hydroxyethyl-acrylate and 2-hydroxyethyl-methacrylate decrease with pH for low pH values before increasing around 8 pH units. Given the strong MT effect caused by the carboxyl groups, and the relatively simple pH dependence of the MT rate (see Fig. 2), the remainder of this paper will focus primarily on explaining the spin exchange dependencies in the acrylic acid- and methacrylic acid-based gels.

The simplest explanation for the dependence of  $R_1^+$  on carboxyl groups is that the exchangeable protons play a vital role in magnetization transfer. However, since carboxyl groups are also hydrophilic (22), the mechanism by which spin exchange occurs is not certain. What is clear is that it is the intact COOH groups, and not the ionized COO<sup>-</sup> groups (as proposed by Koenig (14) in his studies of proteins), which are the conduits for magnetization transfer in the gels studied in this work. This conclusion follows from the data in Fig. 2, where  $R_1^+$  decreases as the pH, and the COO<sup>-</sup> population, increases.

The presence of carboxyl groups greatly enhances the spin exchange rate. However, modeling this increase in terms of a simple exchange between the free water and the carboxyl protons is inadequate for explaining the measured results. This fact can be seen by considering the amplitude of the fast decay component,  $b_f^+$ , in the limit of large  $k_{mf}$ . Keeping only first-order terms in  $R_{1f}/k_{mf}$ ,  $R_{1m}/k_{mf}$ , and  $k_{fm}/k_{mf}$  in Eq. [3] gives

$$b_f^+ = \left[ \frac{M_f(0)}{M_{f\infty}} - \frac{M_m(0)}{M_{m\infty}} \right] \frac{k_{fm}}{k_{mf}},$$

which has magnitude equal to  $2k_{fm}/k_{mf}$  when the free water pool is perfectly inverted with complete selectivity. Since

$$\frac{k_{fm}}{k_{mf}} = \frac{M_{m\infty}}{M_{f\infty}} = \frac{p_m}{p_f},$$

the ratio of the proton fractions dictates the maximum possible value of  $b_f^+$ . In the acrylic acid/BIS polymer, the chemical composition corresponds to a carboxyl proton fraction

**TABLE 2**  
**Proton Fraction of Monomers**

Monomer	Proton fraction
BIS	0.017
Acrylamide	0.019
Methacrylamide	0.022
Acrylic acid	0.015
COOH group only	0.0038
Methacrylic acid	0.019
COOH group only	0.0032
2-Hydroxyethyl-acrylate	0.019
OH group only	0.0024
2-Hydroxyethyl-methacrylate	0.021
OH group only	

*Note.* To get the combined fraction of the monomer and BIS, add the individual proton fractions. (The error resulting from not including each monomer's contribution to the total number of protons is negligible.) Water makes up the remaining proton fraction.

of 0.0038, an acrylic acid proton fraction of 0.015, and an acrylic acid plus BIS proton fraction of 0.032 (see Table 2). The maximum measured value of  $b_f^+$  is 0.048, a value corresponding to a  $k_{fm}/k_{mf}$  minimum of 0.024. That is, the free water effectively exchanges spins with up to three-quarters of the acrylic acid plus BIS protons. There are not enough carboxyl protons to, by themselves, account for the measured  $b_f^+$ . Instead, the carboxyls likely act mainly as a conduit, allowing the free water to exchange spin with the bulk of the macromolecule.

A second noteworthy result is the qualitative similarity of the  $R_1^+$  and  $R_2$  curves. That is,  $R_1^+$  and  $R_2$  have roughly similar dependencies on chemical composition and chemical dynamics as manipulated by changes in monomer and pH. (Such a similarity in the pH dependencies was also seen by Kucharczyk *et al.* (20) in 1-palmitoyl-2-oleoylphosphatidylcholine linked with either cholesterol or galactocerebroside. Note that this study, like the present work, saw an increase in MT at acidic pH values.) These similar dependencies are consistent with previous observations of the likeness in contrast seen in MT and  $T_2$ -weighted images (23). For the six polymers, all significant changes with respect to changes in pH obey  $8 \leq \Delta R_1^+/\Delta R_2 \leq 12$ . If  $k_{im} \ll k_{if}$ , this result is consistent with a three-pool model with macromolecular and free solvent pool sizes equal to the corresponding number of protons, as determined by chemical composition (see Eqs. [10] and [11] and Table 2).

The trends for  $R_1^-$  are less clear. The most noteworthy result is the increase in the  $R_1^-$  of polymers with carboxyls and the decrease in  $R_1^+$  with increasing pH value. Such a result is consistent with fast exchange (relative to the difference in  $R_1$  values) between the free solvent and a macromol-

ecule with a small  $R_1$  value. The macromolecular  $R_1$  value depends on the structural details of the polymer and therefore this result may be quite different than what would occur in tissue.

In order to make a more quantitative analysis of the data, assumptions about the dependence of the intermediate proton pool on pH need to be made. The simplest model allows for acid/base-catalyzed chemical exchange (as described by Eq. [12]) and no change in the bound water or macromolecular structure as a function of pH. This constancy in bound water and macromolecular structure simplifies the analysis, but may limit its applicability. This point will be examined below.

Following the work of Liepinsh and Otting (9), the chemical exchange rate is given by

$$k_{if} \propto \frac{[H^+]}{1 + 10^{15.7-pK}} + \frac{[OH^-]}{1 + 10^{pK-15.7}}, \quad [12]$$

where  $pK$  refers to the exchanging chemical side group, and the brackets indicate concentration. Using standard results (24),

$$[H^+] = 10^{-pH}, \quad [13]$$

$$[OH^-] = 10^{-14+pH}, \quad [14]$$

$$p_i \propto \frac{1}{1 + 10^{pH-pK}}. \quad [15]$$

In order to account for the measured  $R_1^+ \approx k_{mf, effective}$  in all regimes (see Eq. [6]), a knowledge of  $k_{im}$  as a function of  $k_{if}$  is necessary. The rigid linewidth of the macromolecular pool is an upper limit for  $k_{im}$ , since this linewidth is the maximum rate for spin flips and, therefore, is the largest possible cross-relaxation rate. A second upper limit can be found by assuming that the chemical exchange rate  $k_{if}$  dictates the correlation time of the dipole-dipole interaction. If so, then (13)

$$k_{im} \propto \frac{1}{k_{if}} \left( 1 - \frac{6}{1 + 4\omega_0^2 k_{if}^{-2}} \right). \quad [16]$$

The smaller of these two upper limits dictates  $k_{im}$ .

Substituting Eqs. [12] through [16] into Eq. [5] gives  $R_1^+ \approx k_{mf, effective}$  as a function of pH and the  $pK$  value of the exchanging group. That such an analysis cannot account for the current data is evident by looking (in Fig. 2) at the roughly linear  $R_1^+$  dependence of the carboxyls (acrylic acid and methacrylic acid) on pH. pH enters Eqs. [12] through [16] in logarithmic fashion. Therefore, on a linear exchange rate scale, any significant change should occur in 1 or 2 pH units. Regardless of the  $pK$  value, Eqs. [12] through [16]

cannot account for a linear dependence on pH over 6 pH units, as seen in Fig. 2. A remarkably similar linear dependence has been measured previously in aqueous macromolecular suspensions of polysine (21), which has a carboxyl side group. The spin exchange rate from the free water to the macromolecule was measured via a saturation transfer experiment. The data from that study indicate a roughly linear dependence on pH between 4.3 and 9.5 pH units, qualitatively similar to the acrylic acid curve in Fig. 2. Yet another example of the inability of acid/base-catalyzed chemical exchange to account for MT data is seen in water-ethanol solutions, where the measured exchange rates vary logarithmically with pH and, therefore, cannot account for the measured MT rates seen in egg phosphatidylcholine:cholesterol bilayers (21, 25). This difference between the exchange rates in solutions vs polymers is not surprising, given the restricted geometries and bulk surface charge characteristics of polymers.

There are at least three possible explanations for the linear dependence on pH. First, the association constant for a given site may be dependent on the level of protonation of the other sites on the same macromolecule. The value of  $k_{if}$  is no longer expressed by Eq. [12], but is instead, in general, a function of pH and  $n$  association constants, where  $n$  equals the number of exchangeable sites on the macromolecule (26). In such a situation, the occupancy of any one site is no longer independent of other sites, as chemical affinity is affected by long-range electrostatic effects. An analysis in terms of such multiequilibria constants is beyond the scope of the present work. A second possibility, suggested by a reviewer, is that there is a significant distribution of  $pK$  values, thereby giving the linear dependence. Extending Eqs. [12] and [16] to the case of many  $pK$  values greatly complicates the data analysis and is beyond the scope of this paper. A third possibility, suggested by both reviewers, is that the morphology of the macromolecule is a (complicated) function of pH. Such a structural change may affect the relaxation within the macromolecule and the access of free water to spin exchanging sites. The pH of the gel was manipulated after cross-linking occurred in an attempt to minimize this effect; however, the degree to which changes do occur is unknown. All three of these explanations are consistent with previous studies which indicate that the exchangeable proton population of macromolecules is sometimes roughly linear with pH, such as in the case of polymethacrylic acid (26, 27). An independent measure of COOH protonation may help to determine the molecular mechanisms involved in the measured spin exchange rate.

The effect of pH changes on the amount of water associated with a macromolecule is more complicated, and is beyond the scope of the present work. The amount of bound water is influenced by the electrical state of the macromolecule. To the degree to which bound water is influenced by

the protonation of the chemical side groups, the arguments made above concerning chemical exchange are also relevant in assessing the amount of bound water. That is, it is possible that the linearity in  $k_{if}$  with pH could be accounted for by bound water effects. Note, however, that since water is a charge neutral dielectric, its exchange may scale differently than do the ionic  $H_3O^+$  and  $OH^-$  with respect to the bulk surface protonation. Regardless of whether proton exchange or bound water is the primary MT conduit, our results suggest that a gel polymer system exchanges spin in a qualitatively different way than does a freely accessible, and easily measurable, rapidly rotating molecule.

These results demonstrate that, in systems with similar degrees of immobilization, water proton relaxation is highly dependent on the precise nature of the functional groups and on the pH. Notably, at physiologic pH, MT rates are highly sensitive to the presence of carboxyl groups. Also, an analysis of the data suggests that multiequilibria proton exchange, a wide distribution in surface group  $pK$  values, and/or a macromolecular structural dependence on pH may play a significant role in MT in polymer systems.

#### ACKNOWLEDGMENTS

We thank Julie Hammel, Eric Sayers, Nigel George, and Mike Andrec for helpful discussions concerning acid/base biochemistry. We also thank Dr. Robert Shulman for suggesting the interpretation of the pH data in terms of a charged surface, and Michael Barry of MGS Research Inc. for preparing the samples.

This work was supported by the National Cancer Institute, under Grant CA40675.

#### REFERENCES

1. R. M. Henkelman, X. Huang, Q. Xiang, G. J. Stanisz, S. D. Swanson, and M. J. Bronskill, *Magn. Reson. Med.* **29**, 759 (1993).
2. S. D. Wolff and R. S. Balaban, *Magn. Reson. Med.* **10**, 135 (1989).
3. S. H. Koenig and R. D. Brown III, *Magn. Reson. Med.* **30**, 685 (1993).
4. R. G. Bryant, D. A. Mendelson, and C. C. Lester, *Magn. Reson. Med.* **21**, 117 (1991).
5. H. N. Yeung, R. S. Adler, and S. D. Swanson, *J. Magn. Reson. A* **106**, 37 (1994).
6. T. L. Ceckler and R. S. Balaban, *J. Magn. Reson.* **93**, 572 (1991).
7. J. C. Gore, M. Brown, K. F. Mueller, and W. W. Good, *Magn. Reson. Med.* **9**, 325 (1989).
8. B. P. Hills, *Mol. Phys.* **76**, 489 (1992).
9. E. Liepinsh and G. Otting, *Magn. Reson. Med.* **35**, 30 (1996).
10. R. P. Kennan, K. A. Richardson, J. Zhong, M. J. Maryanski, and J. C. Gore, *J. Magn. Reson. B* **110**, 267 (1996).
11. D. F. Gochberg, R. P. Kennan, and J. C. Gore, *Magn. Reson. Med.* **38**, 224 (1997).
12. H. T. Edzes and E. T. Samulski, *Nature* **265**, 521 (1977).
13. H. T. Edzes and E. T. Samulski, *J. Magn. Reson.* **31**, 207 (1978).
14. S. H. Koenig, *Biophys. J.* **69**, 593 (1995).
15. K. V. Vasavada and J. I. Kaplan, *J. Magn. Reson.* **62**, 37 (1985).
16. F. A. L. Anet and D. J. O'Leary, *J. Magn. Reson.* **86**, 358 (1990).
17. H. Winkler and D. Michel, *Adv. Colloid Interface Sci.* **23**, 149 (1985).
18. B. P. Hills, C. Cano, and P. S. Belton, *Macromolecules* **24**, 2944 (1991).
19. S. H. Koenig, *Magn. Reson. Med.* **20**, 285 (1991).
20. W. Kucharczyk, P. M. Macdonald, G. J. Stanisz, and R. M. Henkelman, *Radiology* **192**, 521 (1994).
21. T. L. Ceckler, S. D. Wolff, V. Yip, S. A. Simon, and R. S. Balaban, *J. Magn. Reson.* **98**, 637 (1992).
22. H. J. C. Berendsen, in "Water: A Comprehensive Treatise," Vol. 5, "Water in Disperse Systems" (F. Franks, Ed.), p. 302, Plenum, New York (1975).
23. J. I. Tantt, R. E. Sepponen, R. J. Foust, and E. Kinnunen, "MR of Multiple Sclerosis Plaques at 0.1T: Correlation between Magnetization Transfer Contrast, T1p-Dispersion and Intensity in T2 Weighted Images," p. 356, Society of Magnetic Resonance in Medicine, Berkeley, California (1990).
24. L. Stryer, in "Biochemistry," p. 39, Freeman, New York (1981).
25. A. Knüttel and R. S. Balaban, *J. Magn. Reson.* **95**, 309 (1991).
26. C. Tanford, in "Physical Chemistry of Macromolecules," Wiley, New York (1961).
27. R. Arnold and J. T. G. Overbeek, *Recl. Trav. Chim. Pays-Bas* **69**, 192 (1950).
28. W. H. Press, S. A. Teukolsky, W. T. Vetterling, and B. P. Flannery, "Numerical Recipes in C: The Art of Scientific Computing," 2nd ed., Cambridge Univ. Press, Cambridge (1992).